P2.11 EFFECTS OF MOISTURE ON BAROCLINIC LIFECYCLES

Maurizio Fantini *
ISAC-CNR, Bologna, Italy †

1 INTRODUCTION

In a recent paper (Fantini, 1999a) the linear modes of instability of the Eady problem (Eady, 1949) were studied in dry and moist (saturated) conditions, and results were given for the growth rates and wavelength of the unstable modes.

The moisture representation was obtained from the Emanuel et al (1987) semi-geostrophic model, reformulated for the primitive equations, and amounts to using a reduced static stability for all ascending motion, accounting in this way for the acceleration imposed on rising air by the release of latent heat.

This boring pursuit is now extended to the modes growing on a zero PV jet (Hoskins and West, 1979) in an f-plane model of the troposphere, bounded above by a rigid lid and periodic in both horizontal directions.

The more structured base state has the advantage (with respect to Eady's) of a closer resemblance to atmospheric mean zonal states, and the most unstable modes give rise, when followed in the non linear regime, to a well defined phase of growth followed by decay, instead of the continued exponential growth of the 2D Eady modes, which do not interact with the base state.

A classification of baroclinic lifecycles as seen in numerical experiments with a GCM was given by Thorncroft at al (1993). In this paper we will reproduce the characteristics of LC1, although in simplified geometry, and study how they are modified by release of latent heat in the rising-air sector of the cyclone.

Given the simplified moisture representation and the implied assumption of saturation of ascending air throughout the lifecycle, the diabatic effects here reproduced will be enhanced in comparison with what can be expcted in the atmosphere. At the same time it is hoped that their detection and interpretation will be made easier by the idealized setup of the model.

Simulations of moist baroclinic cyclones, but performed with a more complex GCM and a climatological mean state, were presented recently by Gutowski et al (1992).

*m.fantini@isac.cnr.it
†ISAC-CNR, via Gobetti 101, I-40129 Bologna, Italy

2 MODEL

The numerical model is essentially as described in Fantini (1999a). The incompressible, Boussinesq, primitive equations are integrated on a doubly periodic f-plane, bounded at $z = 0$ and H by rigid lids.

The prognostic equations are written for the deviations u, v and θ from an initial mean zonal state $\bar{u}(y,z), \bar{\theta}(y,z)$.

The buoyancy term in the thermodynamic equation is defined following Emanuel et al (1987), adapted to primitive equations. The final form of static stability in the moist runs is

$$N^2 = \begin{cases} \dfrac{g}{\theta_0}\left(\bar{\theta}_z + \theta_z\right) & \text{where } w < 0 \\ \dfrac{\bar{u}_z^2}{1 - \dfrac{\bar{u}_y}{f_0}} + C\,\theta_{ez} & \text{where } w > 0 \end{cases}$$

where the perturbed part $C\theta_{ez}$ is discussed in Fantini (1999b) while the mean part is derived fron the assumption that a slantwise convective adjustment has occurred on time scales shorter than the baroclinic ones, and reduced to zero the mean moist potential vorticity:

$$\bar{q}_e \equiv \bar{\theta}_{ey}\bar{u}_z + \bar{\theta}_{ez}\left(f_0 - \bar{u}_y\right) = 0$$

The horizontal gradients of saturated equivalent potential temperature θ_e are related to the dry ones by a relation

$$\theta_y = C\theta_{ey}$$

derived originally in Emanuel (1986), and the coefficient has approximately the value $C \simeq 0.6$ for the base state we use.

The base state is a zero-PV jet of the family used by Hoskins and West (1979)

$$\bar{u}(y,z) = \frac{\Delta U}{2}\left[\frac{z}{H} - \frac{\sinh\left(\dfrac{2\Pi N}{f_0 L_y}z\right)}{\sinh\left(\dfrac{2\Pi N}{f_0 L_y}H\right)}\cos\left(\frac{2\Pi}{L_y}y\right)\right]$$

with the geostrophically balanced potential temperature added to a linear stratification $\theta_0\left(1 + (N/g)z\right)$

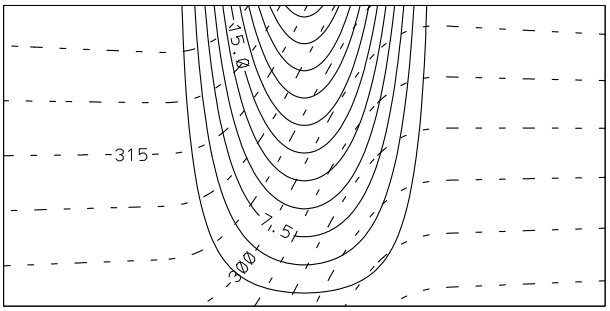

Figure 1: The initial mean zonal state. Solid lines are contours of zonal wind, dashed ones potential temperature

The meridional scale of the jet L_y is chosen at half the size of the domain of integration, to avoid spurious boundary effects in the evolution of the eddies. Figure 1 shows $\bar{u}$ (solid) and $\bar{\theta}$ (dashed) on the mean meridional plane (y, z)

3 PRELIMINARY RESULTS

We show here the evolution of the 6,000 km baroclinic wave, obtained initializing the experiments with a linear normal mode of the dry problem. The 6,000 km wavelength is not the most unstable for either the dry or the moist linear problem, but they are close enough in growth rate that the fundamental wavelength is maintained in a lifecycle run (200 simulated hours), although in the moist run there are hints of shorter scale structures trying to appear. The experiments are run in a 12,000 km periodic domain, so the 6-, 4- and 3-thousand km waves, among the unstable ones, can grow in the model. Fig. 2 shows the evolution of the pressure and potential temperature fields, at the lowest internal level of the model, located at 454 m above ground in the present setup, in the dry case.

The evolution of a baroclinic wave of the same fundamental length in saturated air, shown in Fig. 3 exhibits a stronger cyclone- anticyclone asymmetry, and an elongated warm front with a bent-back curvature.

At higher levels the perturbation appears confined to the northern side of the initial jet (not shown), in coincidence with the reformed jet and baroclinic zone that can be seen in Fig. 4.

In the course of its growth the simulated baroclinic cyclone displays a realistic frontal evolution (see e.g. Shapiro and Keyser, 1990, for a review) including frontal fracture and warm core seclusion. Release of latent heat during the development produces stronger fronts, especially aloft. In most cases the moist cy-

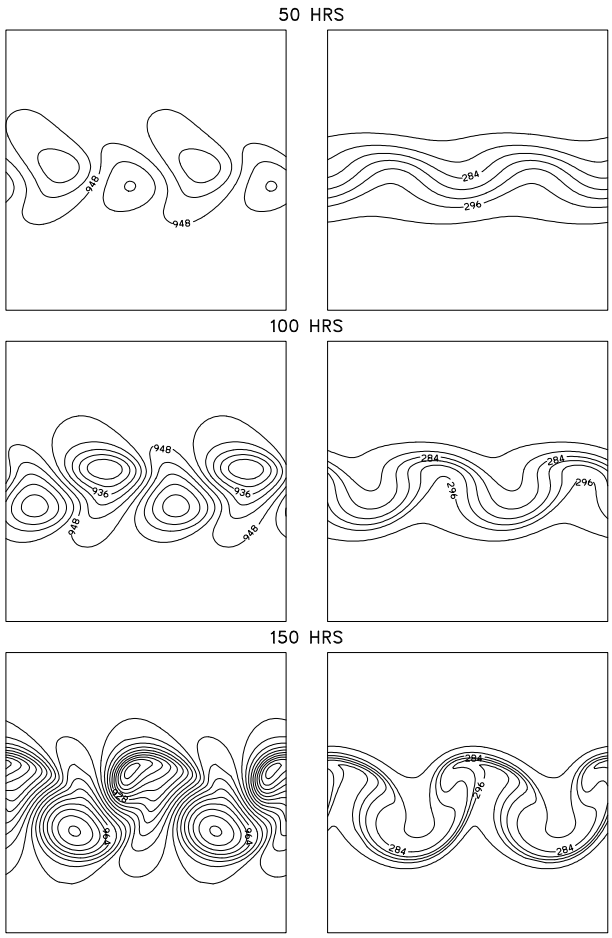

Figure 2: Time evolution of fields of pressure at 454 m (left; contour interval 4 mb) and potential temperature at the same level (right; contour interval 4 K) for the dry experiment. Domain size is 12,000 km in either horizontal direction, 10 km in the vertical

clones also evolve a bent-back warm front, when the dry ones always have the opposite curvature.

At the end of the life cycle, in the dry case, the zonal mean state has much reduced baroclinicity, and two weak areas of meridional temperature gradient lie at the sides of the original jet, in coincidence with the latitudes of predominant zonal orientation of the fronts. In the moist case there is a net asymmetry between the northern side of the original baroclinic zone, where a strong jet is reformed and the cyclone maintains a deep vertical structure, and the southern side, where all baroclinicity has been exhausted and the perturbation is shallow.

The moist life cycle appears to go through two separate stages (see the growth rates in Fig. 5), the first of them not too dissimilar from the dry one, except for the faster development and relatively minor structural modifications, and a second one which feeds on

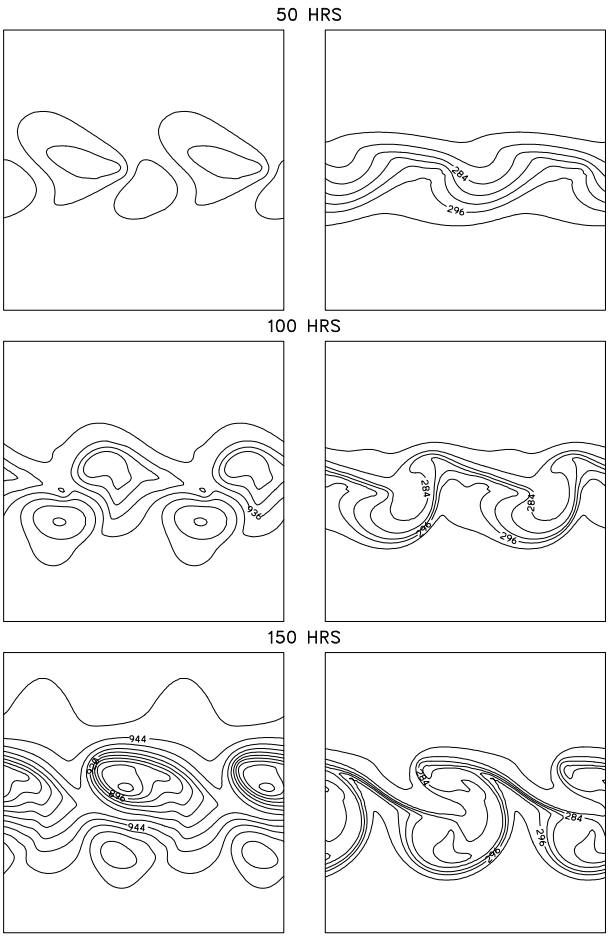

Figure 3: Time evolution of fields of pressure at 454 m (left; contour interval 8 mb) and potential temperature at the same level (right; contour interval 4 K) for the moist experiment

the reformed baroclinic zone after a slow-down phase. It is possible that the intermediate phase of slower growth is only due to our lack of representation of the intermediate range of wavelength, and that the late faster growth coincides with a most unstable wave being finally excited. It is however clear from vertical cross sections of the cyclones (not shown) that in the later phase of growth the moist cyclone has a very shallow structure in the southern part of the domain, and it is only deep in coincidence with the northern baroclinic zone.

We also show in Fig. 6 the ratio R of the energy conversion terms $\overline{w'\theta'}\bar{\Theta}_z$ (EAPE $\rightarrow$ EKE) and $\overline{v'\theta'}\bar{\Theta}_y$ (ZAPE $\rightarrow$ EAPE). This ratio, an *eddy mixing slope* normalized with the slope of isentropic surfaces, measures how much of the zonal available potential energy transfered to the eddies is converted into kinetic energy of the eddies. Its value is necessarily less than one for pure baroclinic development, where

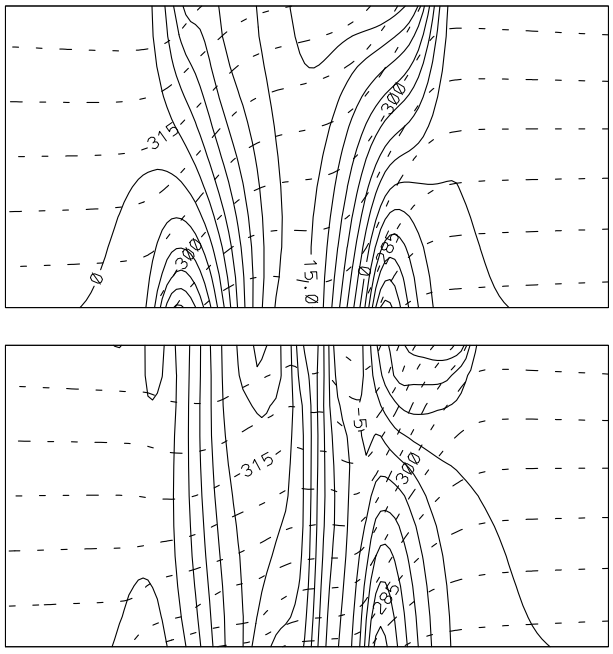

Figure 4: Final (150 hrs) mean zonal states for dry (upper) and moist (lower) experiments

zonal APE is the only source of energy for the eddies. From the numerical results R appears to be nearly constant throughout the dry life cycle, as usually assumed from equipartition arguments. In the course of the moist development R takes different values in the two distinct phases of growth, both larger than the dry counterpart, indicating a more efficient conversion EAPE $\rightarrow$ EKE. At times R becomes larger than one, showing that the EKE for the moist cyclone cannot all be derived from conversion of zonal APE, but that also the energy released by condensation contributes to the KE of the eddies.

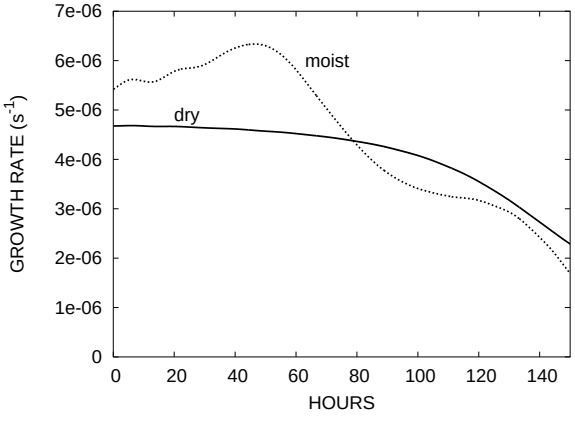

Figure 5: Perturbation growth rate, computed from eddy kinetic energy for dry and moist runs

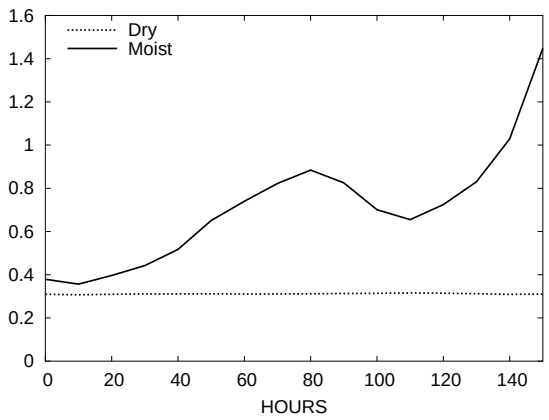

Figure 6: Ratio R of vertical to meridional eddy heat fluxes for dry and moist runs

Finally we show in Fig.7 Ertel potential vorticity near the top for the two cases. The dry one (left panel) exhibits the anticyclonic curvature typical of LC1 (see Thorncroft et al 1993) while the PV anomalies created by the release of latent heat in the moist run modify the PV field in the manner shown in the right panel.

Acknowledgements. This work was supported by MIUR Special Project SINAPSI/ Ecosistemi Marini. http://sinapsi.cineca.it

References

Eady, E. T., 1949: Long waves and cyclone waves. *Tellus*, **1**, 33 – 52

Emanuel, K. A., 1986: An air-sea interaction theory for tropical cyclones. Part I: Steady state maintenance. *J. Atmos. Sci.*, **43**, 585 – 604

Emanuel, K. A., M. Fantini and A. J. Thorpe, 1987: Baroclinic instability in an environment of small stability to slantwise moist convection. Part I: Two-dimensional models. *J. Atmos. Sci.*, **44**, 1559 – 1573

Fantini, M., 1999a: Linear evolution of baroclinic waves in saturated air. *Quart. J. Roy. Meteor. Soc.*, **125**, 905 – 923

Fantini, M., 1999b: Evolution of moist baroclinic normal modes in the nonlinear regime. *J. Atmos. Sci.*, **56**, 3161 – 3166

Gutowski, W. J., L. E. Branscome and D. A. Stewart, 1992: Life cycles of moist baroclinic eddies. *J. Atmos. Sci.*, **49**, 306 – 319

Hoskins, B. J. and N. V. West, 1979: Baroclinic waves and frontogenesis. Part II: Uniform potential vorticity jet flows – cold and warm fronts. *J. Atmos. Sci.*, **36**, 1663 – 1680

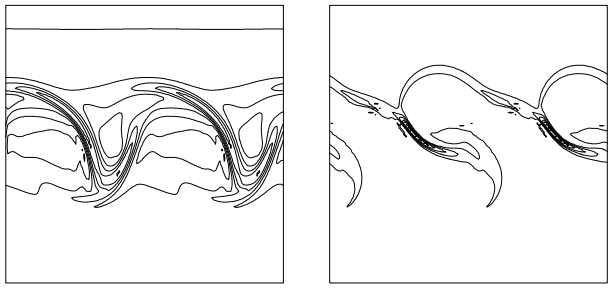

Figure 7: Ertel potential vorticity near the top for dry (left) and moist (right) runs at the last times of Fig.s 2 and 3 respectively

Shapiro, M. A. and D. Keyser, 1990: Fronts, jet streams and the tropopause. *Extratropical Cyclones: The Eric Palmén Memorial Volume. C. W. Newton and E. O. Holopainen Ed.s, American Meteorological Society, Boston*, , 167 – 191

Thorncroft, C. D., B. J. Hoskins and M. E. McIntyre, 1993: Two paradigms of baroclinic-wave lifecycle behaviour. *Quart. J. Roy. Meteor. Soc.*, **119**, 17 – 55